

## MORPHOLOGY AND SPUTTERING OF TUNGSTEN NITRIDES COATINGS EXPOSED TO DEUTERIUM PLASMA

*G.D. Tolstolutsкая, A.S. Kuprin, A.V. Nikitin, R.L. Vasilenko*

*National Science Center “Kharkov Institute of Physics and Technology”,  
Kharkiv, Ukraine*

*E-mail: g.d.t@kipt.kharkov.ua*

Processes of sputtering, surface modification and change in the stoichiometric composition of W and WN coatings deposited on stainless steel by cathodic arc evaporation were studied under the influence of low-energy (500 eV/D) deuterium plasma with fluence of  $(1 \dots 4.5) \cdot 10^{24}$  D<sub>2</sub><sup>+</sup>/m<sup>2</sup> at room temperature. The composition of the WN coating changes under the influence of deuterium plasma, its enrichment with tungsten up to 100 % is observed. Results of erosion studies indicated that the sputtering yields for coatings WN and W are  $\sim 2.4 \cdot 10^{-2}$  at./ion and to be systematically higher than the published data which were measured for bulk materials.

PACS: 52.40Hf, 28.52Fa, 68.49Sf, 79.20Rf

### INTRODUCTION

Tungsten has become the main choice for current and future nuclear devices, specially at the divertor, thanks to its favorable thermo-mechanical properties, low sputtering erosion yield, high thermal conductivity and no chemical reaction with hydrogen [1].

Currently, it is believed that because of the high cost of tungsten, the difficulties in machining due to its hardness and brittleness, the unwieldiness and large weight of the structure, it is not economically reasonable to make the first wall of a fusion reactor entirely of tungsten. Tungsten coatings on a stainless-steel substrate can be considered as a good solution in terms of economic and the protection of structural material from interaction with the plasma [2].

Nevertheless, for both solid tungsten and tungsten coatings there are some drawbacks that need to be solved. One of the major problems is the eroded tungsten atoms can enter the plasma core if not sufficiently screened out. An efficient method to reduce tungsten erosion at the divertor consist on the seeding of gas impurities to decrease the temperature of the plasma at this region by atomic radiation.

Different noble gases like Ne and Ar have been tested but the best results have been obtained with N<sub>2</sub> seeding in ASDEX [3] and JET [4] tokamaks. In both devices an overall enhancement of the plasma confinement was also detected. This improvement is caused by the strongly reduced power load to divertor tiles thanks to the low plasma temperature, but also because of the total suppression of W influx into the plasma [5]. This last effect has been ascribed to the development of tungsten nitrides films at the surface of the W tiles.

Recent experiments have shown that tungsten nitride formed on the W surface due to nitrogen gas seeding [6-8] can prevent H diffusion to the first wall. In [8] it was shown that after exposure of tungsten nitride films to H isotopes at 300 K, H isotopes were detected only in the implantation zone and did not diffuse throughout the material.

However, pre-irradiation with nitrogen increased the retention of D on the near-surface layer. Deuterium diffusion out of the sample was shown to decrease and, consequently, D diffusion inward was increased. It is assumed that these phenomena are related to the barrier effect of the N-containing surface layer. This contradictory situation raises a fundamental interest in studying the mechanisms of interaction of H with tungsten nitrides.

There are two ways to obtain tungsten nitrides: by plasma nitriding of tungsten or by direct deposition.

Nitriding: by ion bombardment the nitrogen atoms are implanted into the tungsten surface at a depth depending on the bombarding energy [1, 9, 10]. This is the best method to simulate the tungsten nitrides formation in a nuclear fusion device. At the low energy of the ions at the divertor (10...20 eV) the nitrogen cannot be implanted, but seems to be enough to react with surface tungsten atoms.

Direct deposition: tungsten nitrides films are usually grown by gas methods like Chemical Vapor Deposition (CVD) and Reactive Magnetron Sputtering (RMS) [11-13]. The main advantage of RMS is that it uses only simple gases as nitrogen and argon with solid W acting as cathode, not the dangerous gases usually employed in CVD. However, RMS is very difficult to optimize as the reactive gas nitrogen in this case can poison the cathode. This effect is observed by a decrease of the growth rate and composition of the film when the quantity of the reactive gas is increased over a certain threshold, which could even stop the deposition.

The most fully realized technology is the physical vapor deposition (PVD) technology [14], which creates a dense coating due to the optimization of the deposition process, and the macroparticle filtration deposition system avoids the appearance of inclusions and associated voids [15].

The goal of this work is to experimentally determine the surface morphology changes, sputtering yields of WN coatings that are deposited by the cathodic arc evaporation on stainless steel 410 AISI substrates and

exposed to low-energy deuterium plasma with fluence  $(1...4.5) \cdot 10^{24} \text{ D}_2^+/\text{m}^2$ .

## 1. MATERIALS AND METHODS

A set of tungsten coatings was formed using an physical vapor deposition (PVD) method in a “Bulat-6” system equipped with a W (99.9 %) cathode of 60 mm diameter [16]. WN coatings deposited on the substrates of stainless steel 410 AISI. Chemical composition of martensitic AISI 410S steel in weight % according to ASTM A240: Fe up to 85; Cr 11,5-13,5; Ni up to 0.6; Mn up to 1; Si to 1; C up to 0.08; P up to 0.04; S up to 0.03. The substrate-cathode distance was about 250 mm. A vacuum-arc plasma source with magnetic stabilization of a cathode spot was used. The coatings application parameters are described in [17].

The WN coatings have been irradiated with deuterium ions using glow gas-discharge plasma at 1000 V. The design and principle of operation of the gaseous plasma source used for irradiation of the samples is described in [18].

The erosion yield was primarily evaluated by a mass loss technique. Before and after plasma exposure, the mass of each target was measured by a microbalance system. The erosion rate was calculated from the mass losses and the total deuterium fluence.

Investigations of surface microstructure were performed using scanning electron microscope JEOL JSM-7001F before and after irradiation. Chemical composition of the coatings was determined by energy dispersive X-ray spectroscopy – EDS.

## 2. RESULTS AND DISCUSSION

Fig. 1 shows a view of initial WN coating deposited by CAE on the substrate of stainless steel 410 AISI. The coating thickness is about 4  $\mu\text{m}$ . The surface of the deposited WN coatings is composed of grain-like protrusions. The large island-like grains are further subdivided into cellular subunits (see Fig. 1,a).

WN-coating has near stoichiometric concentration of N  $\sim 50$  at.% according to EDS analysis (see Fig. 1,b) and a microstructure with elements of a cellular subunits (see Fig. 1,c). As reported in [19], it is the tops of the columnar grains that cause island-like protrusions. The structure of WN-coating is dense and without pores (see Fig. 1,c). The dense structure into those coatings may be explained by sufficiently high energy of deposited tungsten ions and by the high degree of plasma ionization relatively to the flow of evaporated material which is characteristic of cathodic arc evaporation method [14].

Only one phase was revealed in the WN coating – hexagonal tungsten nitride WN- $\delta$  (hexagonal system, space group № 187, structural type WC) with crystallite size  $\sim 29.8$  nm and microstrain  $\sim 7.81 \cdot 10^{-3}$  [17].

Fig. 2 shows a SEM image of plasma-induced surface changes in a WN coating bombarded at 300 K with 1 keV  $\text{D}_2^+$  (0.5 keV/D) to  $(2...4.5) \cdot 10^{24} \text{ D}_2^+/\text{m}^2$ .

The evolution of the surface of  $\delta$ -WN coating due to exposure to a deuterium plasma as shown in Figs. 2,a,b is caused by the sputtering process of cellular structure

at an intermediate dose of irradiation up to obtaining needle like morphology at a dose  $4.5 \cdot 10^{24} \text{ D}_2^+/\text{m}^2$ .

Fig. 3,a shows a view of initial WN coatings deposited by CAE on the substrates of stainless steel 410 AISI with a tungsten intermediate layer. SEM fracture cross-section images of this coating is shown in Fig. 3,b. WN coatings have a dense structure and without pores. The coating thickness is about 5  $\mu\text{m}$ . The evolution of the surface of WN coating due to exposure to a deuterium plasma  $1 \cdot 10^{24} \text{ D}_2^+/\text{m}^2$  are caused by the sputtering process (see Fig. 3,c).

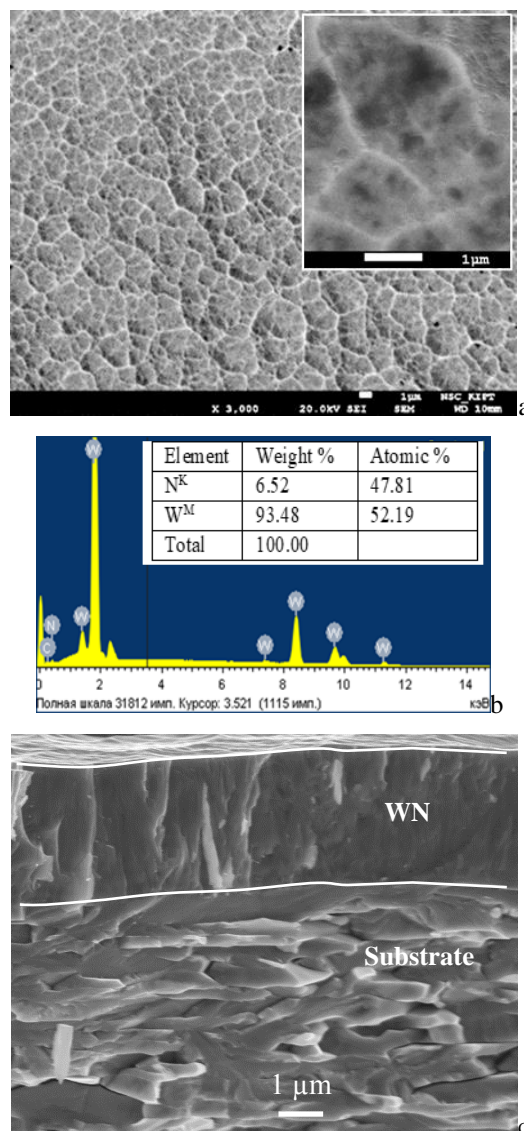


Fig. 1. SEM images of initial surface of WN coating CAE deposited on the substrate of stainless steel 410 AISI (a), EDS X-ray spectrums of surface (b) and SEM fracture cross-section images of WN coating (c)

X-ray EDS spectra of the surface were measured for the initial and plasma-irradiated coatings. Insignificant amounts of impurities (most often on the surface itself) were detected in these measurements. Nevertheless, these impurities were not taken into account in further determining the W:N ratio. For the initial samples the ratio close to stoichiometric about 50 + 50 % is observed. After irradiation this ratio changes (Table 1).

The change of the stoichiometric composition of the coating deposited on a stainless steel substrate is virtually independent of the deuterium fluence. An acceleration of the process of changing the stoichiometry of the coating towards its enrichment with tungsten is observed in the case of coating using an intermediate layer of tungsten.

Thus, the sample exposed to D plasma at 300 K shows a significantly higher W surface concentration than the unexposed sample. This is agreed with the anticipated removal of N from the surface due to D implantation. In ref. [20] based on the available data it was concluded that up to 80 % of the retained D is released as deuterated ammonia or water. These two species cannot be surely distinguished, but it is assumed that ammonia isotopologues dominate. The release of ammonia occurs together with the release of molecular hydrogen.

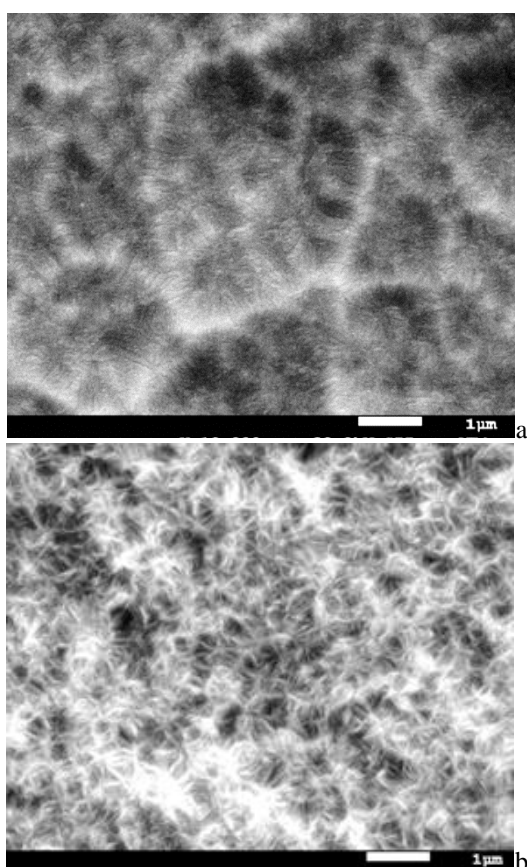


Fig. 2. SEM images of morphology of WN coatings after irradiation at 300 K with 1 keV  $D_2^+$  to  $2 \cdot 10^{24} D_2^+/m^2$  (a) and to  $4.5 \cdot 10^{24} D_2^+/m^2$  (b)

Table 1

W and N fractions before and after exposure to D plasma

Substrate/coating	Dose, $\times 10^{24} D_2^+/m^2$	Element	
		N, at. %	W, at. %
SS/WN <sub>initial</sub>	—	~ 50	~ 50
SS/WN	1	40	60
SS/WN	4	39	61
SS/W/WN <sub>initial</sub>	—	~ 49	~ 49
SS/W/WN	2	25	75
SS/W/WN	3.8	~ 0	~ 100

Table 2 shows the results for the sputtering yields (Y) of W and WN coatings. The sputtering yield was determined from the weight loss and the total deuterium fluence for accordingly 500 eV/D as dominant impinging energy. It should be noted that in this case the number of deuterium particles that fell on the entire sample, not traditionally on the area  $m^{-2}$ , was taken into account.

As seen in Table 2, values of the experimentally measured sputtering yield of the tungsten coatings SS/WN exposed to the D plasma are 1.7 times more than SS/W/WN. For coatings W/WN, there is an almost proportional rise in the sputtering yields with increasing irradiation dose. It should be noted that the W coatings have the sputtering yields which is almost the same as for the coatings WN. However, this value was obtained at a irradiation dose almost four times lower.

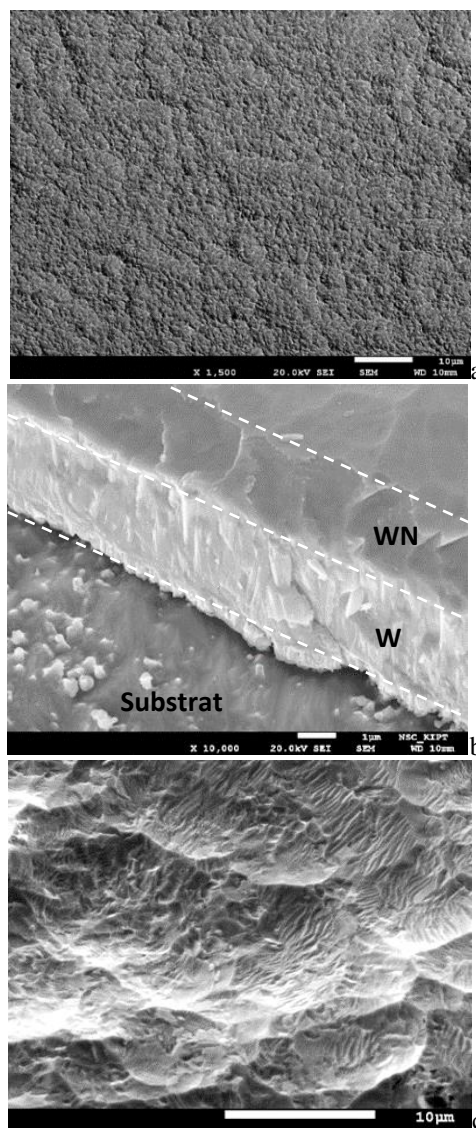


Fig. 3. SEM image of initial surface of WN coatings CAE deposited on the substrate of stainless steel 410 AISI with a tungsten intermediate layer (a), SEM fracture cross-section images of WN coatings (b) and morphology of WN coatings after irradiation at 300 K with 1 keV  $D_2^+$  to  $2 \cdot 10^{24} D_2^+/m^2$  (c)



It is possible that this peculiarity in the sputtering yields of the tungsten coating is related to its structure, which differs significantly from the structure of WN coatings. Fig. 4 shows an SEM image the surface microstructure of the W coatings in the initial state and after exposed to plasma. Initial W coatings exhibit surfaces of densely packed “nanoridges” or overlapping tiles (see Fig. 4,a). Previously reported in [21] that these “nanoridges” were observed on the  $\alpha$ -W phase film surfaces irrespective of the film thickness. The overlapping tiles preferentially sputtered at this dose (see Fig. 4,b).

Table 2  
Sputtering yields of coatings for deuterium (500 eV)

Substrate/coating	Dose, $\times 10^{23}$ D <sub>2</sub> /sample	Y, $\times 10^{-2}$ at./ion
SS/WN	5.5	2.4
SS/WN	6.5	2.4
SS/W/WN	5.6	1.4
SS/W/WN	8.6	2
SS/W	1.5	2.4

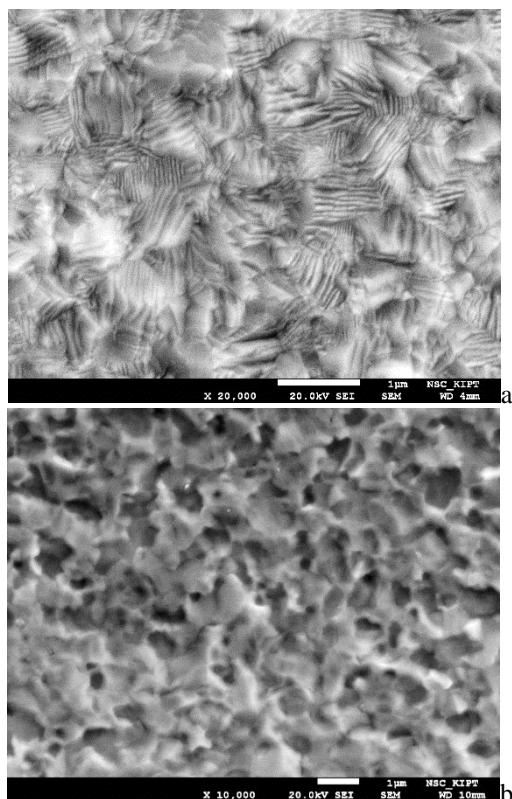


Fig. 4. SEM images of morphology of W coatings in initial state (a) and after irradiation at 300 K with 1 keV D<sub>2</sub><sup>+</sup> to 1.5·10<sup>23</sup> D<sub>2</sub><sup>+</sup> on surface of sample (b)

A comparison of the surface morphologies of the coatings in Figs. 1, 3, 4 shows that the surface roughness is greatest in the case of the tungsten coating. In [22], it is noted that under the current experimental parameters, with the increase of the initial surface roughness, the sputtering morphology and the surface roughness of CLF-1 steel changed to different degrees after erosion of D, which eventually led to the increase of the sputtering rate. The effect of incident D-plasma angle on the sputtering and

redeposition behaviour of the material may explain this phenomenon. Besides, both the specific surface area of the contact plasma and the erosion behaviour of the material by D-plasma increased with the original surface roughness.

Figs. 5,a,b shows respectively SEM top view and cross-section micrographs of a W/WN coatings. There are few agglomerations pyramid-like in the surface possibly increase the surface roughness. The pyramid is a drop of cathode material with tungsten nitride deposited on it (see Fig. 5,c). Fig. 5,d shows the beginning of pyramid sputtering and crater formation after it falling out at fracture.

Sputtering yields of RAFM-related materials, in particular W, by energetic D ion bombardment were measured by means of the thin film technique under well-defined laboratory conditions [23]. The bombardment energy ranged from 60 to 2000 eV/D, which is important in modeling the interaction of ions with material in fusion devices. Comparison with published data for W shows that the here presented data agree with the published data within the experimental un-certainties; however, the yields for sputter-deposited films seem to be systematically higher than the published data which were measured for bulk materials. The authors were unable to determine whether this is a real effect or an experimental error.

In ref. [24] commented, interest in tungsten nitrides is due to its lower tungsten sputtering rate compared to pure tungsten in a nuclear fusion device. Tungsten is sputtered mainly by impurities as the sputtering threshold for hydrogen isotopes and helium ions is more than 100 eV. This is especially evident at the strike points in the divertor region, where energies lower than 100 eV and fluxes in the order of 10<sup>24</sup> ion/m<sup>2</sup>s are expected. The content of some intrinsic impurities N, O and C is reduced by the use of getters, as beryllium in ITER. But the bombardment of other wall materials, as the getters themselves, is unavoidable, and could lead to an excessive sputtering, especially when the so-called self-sputtering with tungsten atoms occurs. sputtering: A decrease in the tungsten atom physical sputtering is expected due to the accumulation of nitrogen at the surface, its preferential sputtering, and the similar bonding energy between NW and WW.

Chemical sputtering of nitrogen by hydrogen is confirmed by the production of ammonia, not only during N<sub>2</sub> seeded pulses but also during subsequent non-seeded ones [11]. In this way the equilibrium between wall nitrogen implantation and erosion by hydrogen in conditions similar to those of ITER is expected to occur in the initial 0.1...1 s of the discharge [9].

Few works have been devoted to the study of nitrogen erosion from tungsten nitrides by hydrogen plasma [9]. N was implanted at 2.5 keV, and the saturation was reached at 2.3·10<sup>20</sup> N/m<sup>2</sup> with an implantation thickness of 10 nm. That film presented a decrease of sputtering yield with 5 keV Ar close to the estimated by SDTRIM.SP. Oppositely, the sputtering yield with deuterium at 2.5 keV was half than predicted: around 0.022...0.044. Although the code correctly models dynamic retention, the value of the experimentally measured erosion was even smaller than the code predicted. SDTRIM.SP was also used to estimate the W sputtering decrease with different % N in a D plasma. For pure N plasma a decrease of 30 % of W erosion is observed. Therefore, experiments at fluence, and

if possible, fluxes equivalent to the ones expected in ITER are highly desirable, as the material degradation changes drastically with both parameters.

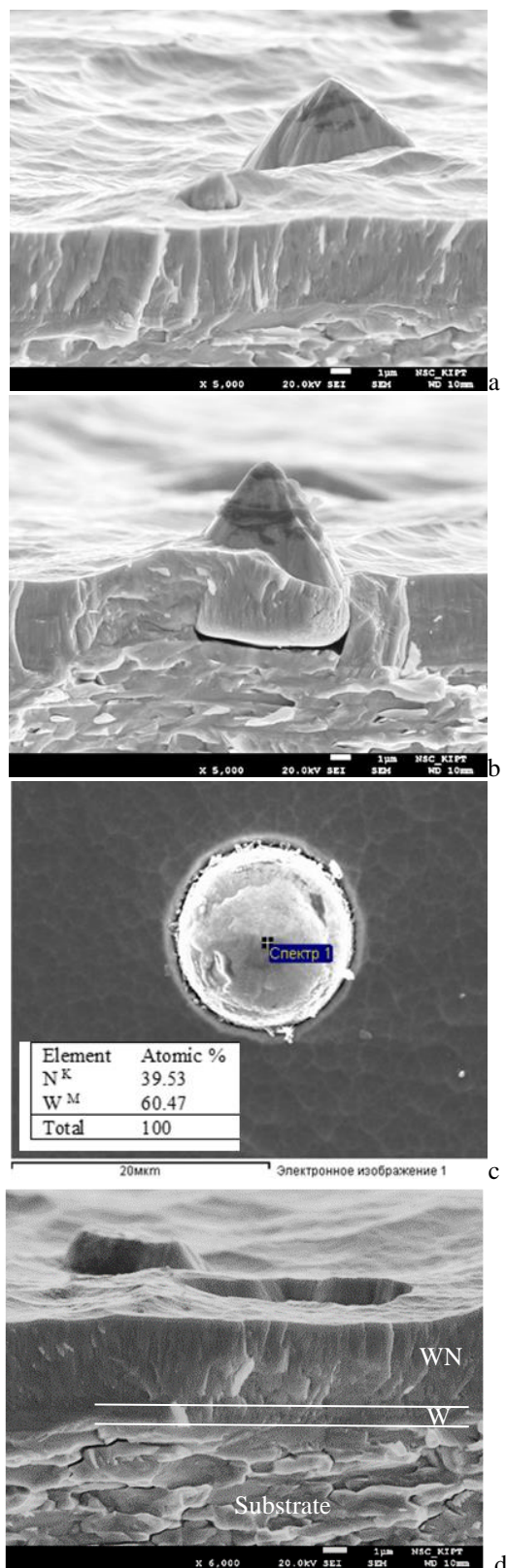


Fig. 5. SEM fracture cross-section images of W/WN coatings (a, b), EDS X-ray spectrums of surface pyramid-like agglomeration (c) and morphology of WN coatings after irradiation at 300 K with 1 keV  $D_2^+$  to  $1 \cdot 10^{24} D_2^+/m^2$  (d)

The microstructures, the behavior of H in  $W_2N_1$ ,  $W_1N_1$  and  $W_2N_3$  during dissolution, diffusion and retention have been systematically studied by theoretical calculations [25]. It was found that the H atom prefers to dissolve in tungsten nitride compounds than in the W crystal under the same conditions. Tungsten nitride compounds play the role of a holding element due to the formation of strong N-H bonds after the dissolution of the H atoms in the compounds. Moreover, the H atoms do not form  $H_2$  molecules at vacant sites. It has been demonstrated that tungsten nitride films, which can form on top of the first wall W due to nitrogen gas seeding or can be deposited on top of the first wall W experimentally, significantly reduce hydrogen retention in the first wall W.

## CONCLUSIONS

Processes of sputtering, surface modification and change of the stoichiometric composition of W and WN coatings deposited on stainless steel by cathodic arc evaporation were studied under the influence of low-energy (500 eV) deuterium plasma with fluence of  $(1 \dots 4.5) \cdot 10^{24} D_2^+/m^2$  at room temperature. All deposited coatings having dense microstructure without pores.

Initial WN-coating has near stoichiometric concentration of N ~ 50 at. % and a microstructure with columnar structure elements.

The stoichiometric ratio of W:N is close to about 50 : 50 % for the initial coating. The change of the stoichiometric composition of the WN coatings on SS is almost (~ 40 at. % N : 60 at. % W) independent on the deuterium fluence in range of  $(1 \dots 4) \cdot 10^{24} D_2^+/m^2$ . A tungsten enrichment up to 100 at. % is observed for SS/W/WN coatings.

The experimentally measured sputtering yield of the tungsten coatings SS/WN exposed to the D plasma are 1.7 times more than for SS/W/WN and is  $2.4 \cdot 10^{-2}$  at./ion and  $1.4 \cdot 10^{-2}$  at./ion, respectively. For coatings W/WN, there is an almost proportional rise of the sputtering yields with an increasing of fluence. A sputtering yield of W coatings is higher compared to WN and bulk tungsten coatings, which may be due to an increase of the initial surface roughness of W coatings.

## ACKNOWLEDGEMENTS

The work was financially supported by the National Academy of Science of Ukraine and The European Federation of Academies of Sciences and Humanities (ALLEA), within the framework the "European Fund for Displaced Scientists", Grant EFDS-FL2-04.

## REFERENCES

1. R.A. Pitts, X. Bonnin, F. Escourbiac, et al. Physics basis for the first ITER tungsten divertor // *Nuclear Materials and Energy*. 2019, v. 20, p. 100696.
2. C. Ruset, E. Grigore, H. Maier, R. Neu, H. Greuner, M. Mayer, and G. Matthews. Development of W coatings for fusion applications // *Fusion Eng. Des.* 2011, v. 86(9-11), p. 1677-1680.

3. K. Schmid, A. Manhard, Ch. Linsmeier, A. Wiltner, T. Schwarz-Selinger, W. Jacob, S. Mändl. Interaction of nitrogen plasmas with tungsten // *Nucl. Fusion*. 2010, v. 50, N 2, p. 025006.
4. S. Brezinsek, A. Kirschner, M. Mayer, et al. Erosion, Screening, and Migration of Tungsten in the JET Divertor // *Nuclear Fusion*. 2019, v. 59, N 9, p. 096035.
5. R. Neu, A. Kallenbach, M. Balden, et al. Over-view on plasma operation with a full tungsten wall in ASDEX Upgrade // *J. Nucl. Mater.* 2013, v. 483, p. S34-S41.
6. L. Gao, W. Jacob, P. Wang, U. von Toussaint, A. Manhard. Influence of nitrogen pre-implantation on deuterium retention in tungsten // *Phys. Scr.* 2014, v. T159, p. 014023.
7. H.T. Lee, M. Ishida, Y. Ohtsuka, Y. Ueda. The influence of nitrogen on deuterium permeation through tungsten // *Physica Scripta*. 2014, v. T159, p. 014021.
8. L. Gao, W. Jacob, T. Schwarz-Selinger, A. Manhard. Deuterium implantation into tungsten nitride: Negligible diffusion at 300 K // *J. Nucl. Mater.* 2014, v. 451, p. 352-355.
9. G. Meisl, K. Schmid, O. Encke, T. Höschen, L. Gao, Ch. Linsmeier. Implantation and erosion of nitrogen in tungsten // *New Journal of Physics*. 2014, v. 16, p. 093018.
10. H.L. Zhang, D.Z. Wang, N.K. Huang. The effect of nitrogen ion implantation on tungsten surfaces // *Applied Surface Science*. 1999, v. 150, Issues 1-4, p. 34-38.
11. M. Oberkofler, D. Douai, S. Brezinsek, et al. First nitrogen-seeding experiments in JET with the ITER-like Wall // *J. Nucl. Mater.* 2013, v. 438, p. S258-S261.
12. Z. Wang, Z. Liu, Z. Yang, S. Shingubara. Characterization of sputtered tungsten nitride film and its application to Cu electroless plating // *Microelectronic Engineering*. 2008, v. 85, p. 395-400.
13. M.L. Addonizio, A. Castaldo, A. Antonaia, E. Gambale, L. Iemmo. Influence of process parameters on properties of reactively sputtered tungsten nitride thin films // *Journal of Vacuum Science and Technology. A: Vacuum, Surfaces and Films*. 2012, v. 30, p. 031506.
14. I.I. Aksenov, A.A. Andreev, V.A. Belous, V.E. Strel'nitskij, V.M. Khoroshikh. *Vacuum arc: plasma sources, deposition of coatings, surface modification*. Kiev: "Naukova Dumka", 2012.
15. A. Kuprin, V. Belous, V. Voyevodin, V. Bryk, R. Vasilenko, V. Ovcharenko, E. Reshetnyak, G. Tolmachova, P. V'yugov. Vacuum-arc chromium-based coatings for protection of zirconium alloys from the high-temperature oxidation in air // *J. Nucl. Mater.* 2015, v. 465, p. 400-406.
16. A.S. Kuprin, S.A. Leonov, V.D. Ovcharenko, E.N. Reshetnyak, V.A. Belous, R.L. Vasilenko, G.N. Tolmachova, V.I. Kovalenko, I.O. Klimenko. Deposition of TiN-based coatings using vacuum arc plasma in increased negative substrate bias voltage // *Problems of Atomic Science and Technology. Series "Plasma Electronics and New Methods of Acceleration"* (123). 2019, № 5, p. 154-160.
17. G.D. Tolstolutsкая, A.S. Kuprin, A.V. Nikitin, et al. Deuterium trapping and sputtering of tungsten coatings exposed to low-energy deuterium plasma // *Problems of Atomic Science and Technology. Series "Physics of Radiation Effect and Radiation Materials Science"* (126). 2020, № 2, p. 54-59.
18. A.V. Nikitin, G.D. Tolstolutsкая, V.V. Ruzhytskyi, V.N. Voyevodin, et al. Blister formation on 13Cr2MoNbVB ferritic-martensitic steel exposed to hydrogen plasma // *J. Nucl. Mater.* 2016, v. 478, p. 26-31.
19. Y. Denga, S. Yin, Y. Hong Yi, et al. Microstructures and properties of novel nanocomposite WN<sub>x</sub> coatings deposited by reactive magnetron sputtering // *Applied Surface Science*. 2020, v. 512, p. 145508.
20. L. Gao, W. Jacob, G. Meisl, T. Schwarz-Selinger, T. Höschen, U. von Toussaint, T. Dürbeck. Interaction of deuterium plasma with sputter-deposited tungsten nitride films // *Nucl. Fusion*. 2016, v. 56, p. 016004.
21. H. Brune. Microscopic view of epitaxial metal growth: nucleation and aggregation // *Surface Science Reports*. 1998, № 31, v. 4-6, p. 121-229.
22. L. Qiao, P. Wang, M. Hu, L. Gao, W. Jacob, E.G. Fu, G.N. Luo. Erosion and deuterium retention of CLF-1 steel exposed to deuterium plasma // *Physica Scripta*. 2017, v. T170, p. 014025.
23. K. Sugiyama, K. Schmid, W. Jacob. Sputtering of iron, chromium and tungsten by energetic deuterium ion bombardment // *Nuclear Materials and Energy*. 2016, v. 8, p. 1-7.
24. D. Alegre, T. Acseente, A. B. Martin-Rojo, et al. Characterization of tungsten nitride layers and their erosion under plasma exposure in NANO-PSI // *Romanian Reports in Physics*. 2015, v. 67, № 2, p. 532-546.
25. X.B. Ye, B.C. Pan. The mechanism on retention of hydrogen in three representative tungsten nitride compounds in nuclear fusion reactors // *J. Nucl. Mater.* 2021, v. 544, p. 152687.

*Article received 10.01.2023*

### **МОРФОЛОГІЯ ТА РОЗПИЛЕННЯ ПОКРИТТІВ З НІТРИДУ ВОЛЬФРАМУ ПІД ВПЛИВОМ ДЕЙТЕРІЄВОЇ ПЛАЗМИ**

*Г.Д. Толстолюцька, О.С. Купрін, А.В. Нікітін, Р.Л. Василенко*

Досліджено вплив низькоенергетичної (500 eV/D) дейтерієвої плазми з флюенсом  $(1..4,5) \cdot 10^{24} \text{ D}_2^+/\text{m}^2$  за кімнатної температури на процеси розпилення, модифікацію поверхні та зміну стехіометричного складу покриттів W і WN, осаджених на нержавіючу сталь катодним дуговим випаровуванням. Опромінення дейтерієвою плазмою змінює склад покриття WN, спостерігається його збагачення вольфрамом до 100 %. Результати досліджень ерозії показали, що коефіцієнти розпилення для покриттів WN і W становлять  $\sim 2,4 \cdot 10^{-2}$  ат./іон і систематично перевищують опубліковані дані для об'ємних матеріалів.